



Research article

Moxibustion alleviates intestinal inflammation in ulcerative colitis rats by modulating long non-coding RNA LOC108352929 and inhibiting Phf11 expression

Guona Li^{a,b,1}, Chen Zhao^{b,c,1}, Jing Xu^{a,1}, Yan Huang^c, Yu Qiao^c, Feng Li^c, Guangbin Peng^a, Shiyu Zheng^a, Lu Zhu^a, Ling Yang^c, Zhaoqin Wang^{a,c,*}, Huangan Wu^{a,c,**}

^a Yueyang Hospital of Integrative Chinese and Western Medicine, Shanghai University of Traditional Chinese Medicine, Shanghai, 200437, China

^b School of Acupuncture-Moxibustion and Tuina, Shanghai University of Traditional Chinese Medicine, Shanghai, 201203, China

^c Shanghai Research Institute of Acupuncture and Meridian, Shanghai University of Traditional Chinese Medicine, Shanghai, 200030, China

ARTICLE INFO

Keywords:

Ulcerative colitis

Moxibustion

Long non-coding RNA

LOC108352929

Phf11

ABSTRACT

Long noncoding RNA (lncRNAs) are involved in the pathogenesis of ulcerative colitis (UC). Moxibustion, a traditional Chinese medicine, can improve symptoms in patients with UC and reduce intestinal inflammation in rats with UC. However, it remains unclear whether the ameliorative effect of moxibustion on intestinal mucosal inflammation in UC is related to lncRNAs. Thirty-two rats were randomly assigned to four groups: normal control, UC, moxibustion (MOX), and sulfasalazine (SASP). The UC rat model was induced by administering 4% dextran sulfate sodium (DSS) in drinking water. Rats in the moxibustion group underwent bilateral Tianshu (ST25) moxibustion using the herbs-partition moxibustion method. Rats in the sulfasalazine group received SASP solution *via* gavage twice daily for seven consecutive days. Our results revealed that, compared with the UC group [2.00 (1.00, 2.50)], the DAI score [0.25 (0.00, 0.50)] was significantly lower in the MOX group ($P < 0.05$). Compared with the UC group [13.00 (11.25, 14.00)], the histopathological score [5.50 (4.00, 7.75)] was significantly lower in the MOX group ($P < 0.05$). In addition, the CMDI and macroscopic scores were decreased in the MOX group ($P < 0.05$). Moxibustion significantly decreased the protein expression of inflammatory factors TNF- α , IFN- γ , and IL-1 β in the colonic tissues of UC rats ($P < 0.05$), thereby suppressing the inflammatory response. Moreover, moxibustion exerted a regulatory influence on colon lncRNA and mRNA expression profiles, upregulating LOC108352929 and downregulating Phf11 in rats with UC ($P < 0.05$). Moxibustion also led to a reduction in the expression and colocalization of Phf11 and NF- κ B in the colons of UC rats. Moreover, knockdown of LOC108352929 in rat enteric glial cells demonstrated a significant upregulation of TNF- α mRNA expression ($P < 0.05$). In summary, these data illustrate that moxibustion effectively ameliorates DSS-induced colonic injury and inflammation while exerting regulatory control over the lncRNA-mRNA co-

* Corresponding author. Yueyang Hospital of Integrative Chinese and Western Medicine, Shanghai University of Traditional Chinese Medicine, Shanghai, 200437, China.

** Corresponding author. Yueyang Hospital of Integrative Chinese and Western Medicine, Shanghai University of Traditional Chinese Medicine, Shanghai, 200437, China.

E-mail addresses: wangzhaoqin@fudan.edu.cn (Z. Wang), wuhuangan@shutcm.edu.cn (H. Wu).

¹ These authors contributed equally to this work.

<https://doi.org/10.1016/j.heliyon.2024.e26898>

Received 5 November 2023; Received in revised form 9 February 2024; Accepted 21 February 2024

Available online 23 February 2024

2405-8440/© 2024 Published by Elsevier Ltd.

This is an open access article under the CC BY-NC-ND license

(<http://creativecommons.org/licenses/by-nc-nd/4.0/>).

expression network in UC rats. Collectively, the *in vivo* and *in vitro* studies suggested that LOC108352929-Phf11 may serve as a potential biological marker for moxibustion in the treatment of UC.

1. Introduction

Ulcerative colitis (UC) is a recurrent and remitting inflammatory bowel disease (IBD) that primarily affects the colonic and rectal mucosae, making it a challenging clinical condition. The precise etiology of UC remains incompletely understood, as its development is influenced by various factors, including compromised intestinal mucosal barriers, disruptions in immune responses within colonic mucosal tissues, intestinal flora dysbiosis, environmental elements, and genetic predisposition [1]. Moreover, the global incidence of UC is on the rise [2], with a notable 1.5 to nearly 20-fold increase in the incidence and prevalence in some Asian countries [3]. This surge in prevalence has resulted in a substantial increase in UC-related healthcare expenditures. Therefore, it is imperative to identify safe, effective, and cost-efficient treatments.

Long non-coding RNA (lncRNA) is a class of non-coding RNAs with a length exceeding 200 nucleotides that significantly influence various biological processes, such as chromosomal silencing, chromatin modification, transcriptional activation, transcriptional interference, and intranuclear transport [4]. Previous studies have demonstrated a close association between aberrant lncRNA expression and the pathogenesis of UC [5]. Notably, extensive dysregulation of both lncRNA and protein-coding gene expression is observed in the colonic tissues of patients with active and inactive UC [6]. Furthermore, certain specific lncRNA can mitigate colonic ulcers in UC rats by elevating the expression of cytokines such as IL-10 [7].

Moxibustion is a traditional Chinese medicine that achieves its therapeutic effects by burning moxa floss at specific acupoints. We have previously demonstrated that moxibustion can effectively ameliorate colonic mucosal injuries, reduce chronic mucosal inflammation, and accelerate ulcer healing in both UC patients and rat models [8,9]. Given the pivotal roles of lncRNAs in various diseases, moxibustion has shown promise for the treatment of conditions, such as Crohn's disease and adjuvant arthritis by modulating lncRNA expression [10,11]. However, to date, no studies have explored the modulatory effects of moxibustion on intestinal mucosal immunity in rats with UC from the perspective of lncRNA modification. Therefore, this study aimed to assess the regulatory effects of moxibustion on the intestinal lncRNA and mRNA expression profiles in rats with UC using RNA-sequencing techniques. In the present study, we identified numerous differentially expressed lncRNAs and mRNAs. Among the paired lncRNAs and mRNAs, moxibustion had a significant regulatory effect on LOC108352929-Phf11.

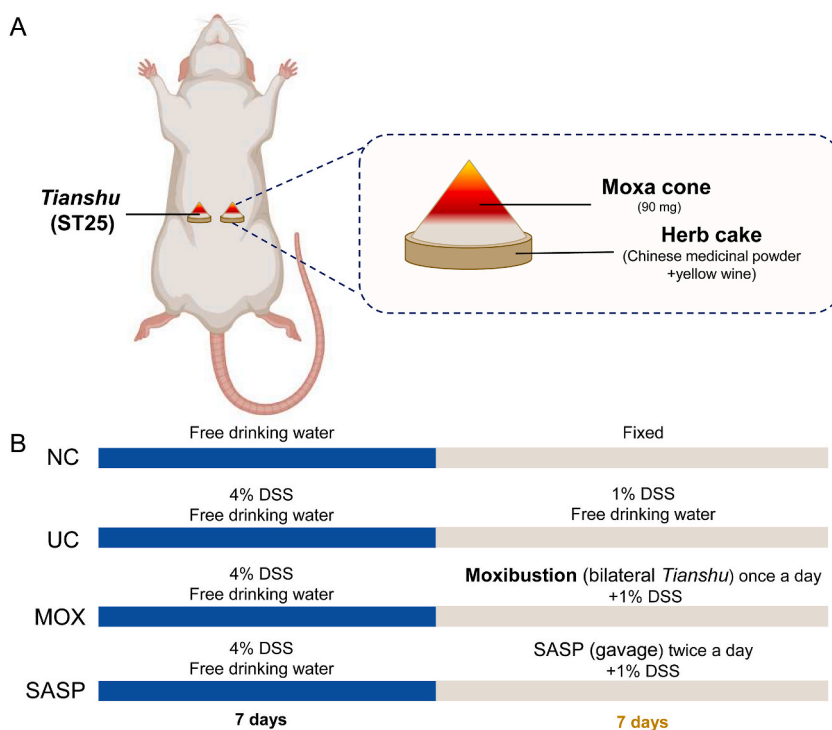


Fig. 1. Flowchart of this experiment. (A) Schematic diagram of moxibustion treatment; (B) Operations performed in each group of rats. NC: the normal control group; UC: the ulcerative colitis model group; MOX: the moxibustion group; SASP: the sulfasalazine group.

2. Materials and methods

2.1. Animals

All animal experiments were conducted according to the guidelines and regulations established by the Animal Ethics Committee of Shanghai University of Traditional Chinese Medicine (approval reference PZSHUTCM200209001). A total of 32 male Sprague-Dawley rats, with an average weight of 180 ± 20 g, were procured from Shanghai Slac Co (production license number: SYXK (Shanghai) 2014-0008). These rats were accommodated at the Shanghai University of Traditional Chinese Medicine's Experimental Animal Center, where the environmental conditions were maintained at a constant room temperature of 20 ± 2 °C, with a 12-h day-night cycle, and a relative humidity range of 50%–70%.

2.2. Establishment of the UC rat model

After a one-week acclimatization period, the rats were randomly assigned to four groups: normal control group (NC), ulcerative colitis model group (UC), moxibustion group (MOX), and sulfasalazine group (SASP), with eight rats in each group. An experimental ulcerative colitis model was induced by administering 4% dextran sulfate sodium (DSS; 9011-18-1, MP Biomedical, USA) in sterile drinking water for 7 days. Subsequently, the UC, MOX, and SASP groups were maintained with 1% DSS for modeling [12]. The moxibustion and SASP treatments were initiated after the modeling process was completed. Moxibustion was performed on bilateral *Tianshu* (ST25) acupoints. Chinese medicinal powder (Shanghai Huaji Pharmaceutical Co., LTD, China) and yellow wine were used to create herb cakes, each with a diameter of 0.8 cm and a thickness of 0.4 cm. These cakes were placed on the bilateral ST25 acupoints with a moxa cone (approximately 90 mg, Nanyang Hanyi Moxa, China) positioned on top of each cake. Two moxa cones were applied to each acupoint once daily for 7 days (Fig. 1A). The rats in the SASP group were administered intragastrically with SASP solution (Shanghai Zhongxi Sunve Pharmaceutical Co., Ltd., China) twice daily for 7 days. The daily dosage was based on the ratio of 1:0.018 for adults to rats [13]. The NC and UC groups were subjected to the same handling and restraint procedures. An operational flowchart of this experiment is presented in Fig. 1B.

2.3. Disease activity index (DAI)

Stool consistency, body weight, and gross bleeding were observed and recorded, and the DAI score was performed [14]. The scoring criteria were as follows: (a) stool consistency: 0 = normal, 2 = loose stool, 4 = diarrhea; (b) body weight loss: 0 = none, 1 = 1–5%, 2 = 6–10%, 3 = 11–15%, 4 = >15%; and (c) gross bleeding: 0 = normal, 2 = positive occult blood test, and 4 = visible bleeding. The DAI score was calculated as the average of these three values.

2.4. Evaluation of colonic damage

Upon completion of the treatment regimen, the rats underwent a 24-h fasting period without access to water and were subsequently anesthetized via intraperitoneal injection with 2% pentobarbital sodium (40–50 mg/kg). Following successful anesthesia, the abdominal cavity of the rats was surgically opened and the colon was carefully extracted from the pubic symphysis to the cecum. The colon was longitudinally dissected along the mesentery by saline irrigation. Colonic mucosa damage index (CMDI) and macroscopic scores were used to assess the colonic injury. CMDI scoring criteria and scores were as follows: 0 = no inflammation or ulceration; 1 = localized congestion without ulceration; 2 = ulceration without congestion; 3 = ulceration and inflammation at only one site; 4 = inflammation and ulceration at ≥ 2 sites extending >1 cm; 5 = ulceration extending >2 cm [15,16]. The macroscopic score was calculated by observing vascularity, secretions, ulcers, and adhesions [17].

2.5. Hematoxylin-eosin (HE) staining and histopathological scores

Rat colon tissues were dehydrated and fixed in 4% paraformaldehyde. After fixation, the tissues were embedded in paraffin and sectioned into 4 μ m thick slices for hematoxylin-eosin (HE) staining and subsequent pathological examination. Histopathological evaluation of the HE-stained colon specimens included the assessment of ulceration, infiltration of inflammatory cells, hyperplasia of granulation tissue, lesion depth, fibrosis, reduction in goblet cells, presence of crypt abscesses, destruction of mucosal structure, and degree of thickening of the muscular layer [17].

2.6. RNA-sequencing (RNA-seq) and bioinformatics analysis

Colon tissues from three rats in each group were selected for RNA-seq analysis. Total RNA was extracted from colon tissues using a TRIzol kit (15596018, Invitrogen, USA), and sample quality control was conducted using an ND-1000 Nanodrop and Agilent 2200 TapeStation. The paired-end standard sequencing program was executed following the methodological flow of the Illumina platform instruments, and the resulting data underwent bioinformatics analysis upon completion of the run. Differentially expressed lncRNAs and mRNAs between experimental groups were screened based on criteria such as $|\log_2(\text{Fold Change})| > 1$ and $(P < 0.05)$, and their functional pathways were assessed using the Kyoto Encyclopedia of Genes and Genomes (KEGG). To establish the relationship between differentially expressed lncRNAs and mRNAs, the target mRNAs of these lncRNAs were predicted using both *cis*-regulatory (In Cis) and

trans-regulatory (In Trans) approaches. These predictions were performed by referencing the NCBI, RNA Central, and GENCODE databases.

2.7. *LncRNA-miRNA-mRNA network construction*

MiRanda, PITA, and RNAhybrid were employed to predict the recognition elements of lncRNAs in microRNAs (miRNAs), and the shared predictions from these three tools were considered candidate interacting miRNAs for the lncRNAs. TargetScan, MiRanda, MiRWalk, and miRTarBase were used to predict upstream miRNAs of mRNAs from various databases, and the results from the combined predictions of multiple tools were designated as candidate upstream miRNAs of mRNAs. The lncRNA-miRNA-mRNA interaction network was constructed using a combined score threshold > 0.9.

2.8. *RT-qPCR*

RT-qPCR was used to assess the expression of differentially expressed lncRNAs and mRNAs. Total RNA was extracted from colon tissues using a TRIzol kit (15596018, Invitrogen, USA) and quantified using a spectrophotometer; furthermore, RNA was reverse transcribed into cDNA. RT-qPCR was performed using a real-time detector (ABI, USA), Real-time PCR System (Roche, Switzerland), and SYBR Master Mix kit (RR047A, Takara, Japan). The PCR reaction involved a reaction system comprising 1.5 μ l H₂O, 5 μ l 2 \times SYBR GREEN PCR mix, 1 μ l Forward Primer (10 p.m./ μ l), 1 μ l Reverse Primer (10 p.m./ μ l), and 2.5 μ l cDNA template. The reaction conditions were as follows: pre-denaturation at 95 °C for 2 min; denaturation at 95 °C for 5 s; annealing at 60 °C for 10 s; extension at 72 °C for 40 s. This process was repeated 45 times. The obtained data were compared with GAPDH expression levels to calculate Ct values for all genes, which were further quantified by the $2^{-\Delta\Delta Ct}$ methods. The primer sequences for LOC103693584, LOC102547136, LOC108352929, ENSRNOG00000058784.1, Stxbp5l, LOC102549235, Phf11, RT1-N3, and GAPDH are listed in [Supplementary Table S1](#). RT-qPCR was also used to determine the basal expression of lncRNAs LOC108352929 and Phf11 in rat enteric glial cells (EGCs), with the primer sequences provided in [Supplementary Table S2](#). Additionally, RT-qPCR was employed to assess the efficiency of lncRNA LOC108352929 knockdown, as well as the expression of Phf11, TNF- α , and IL-1 β in the cells. The primer sequences used in these experiments are listed in [Supplementary Table S3](#).

2.9. *Western blot*

TNF- α , IFN- γ , and IL-1 β protein expression in the colon tissues of rats in each group were determined using Western blot analysis. Total colon tissue proteins were extracted using RIPA lysis buffer and quantified using a BCA Protein Concentration Assay Kit (SD0012, Simuwubio, China). Equal amounts of proteins were separated by sodium dodecyl sulfate-polyacrylamide gel electrophoresis and subsequently transferred to PVDF membranes. After the transfer, the membranes were placed on a decolorizing shaker and blocked with 5% skim milk for 1 h. Following the blocking step, diluted primary antibodies (TNF- α : ab6671, Abcam, USA, 1:1000; IFN- γ : ab171081, Abcam, 1:3000; IL-1 β : ab254360, Abcam, 1:1000; GAPDH: AF1186, Beyotime, China, 1:2000) were applied and incubated at 4 °C overnight. The protein bands were then subjected to three 5-min washes with TBST on a decolorizing shaker at room temperature. Finally, the protein bands were visualized using a gel imaging system (Bio-Rad, ChemiDosTM XPS +, USA), and the optical density values of the target protein and internal reference bands were analyzed using the Image Lab 4.1 software processing system.

2.10. *Immunofluorescence staining*

Immunofluorescence staining was performed to detect the co-expression of Phf11 and NF- κ B in rat colon tissues. Sections were deparaffinized, rehydrated, and treated according to standard protocols. Next, the sections were washed with PBS and incubated in a blocking buffer at room temperature, shielded from light, for 25 min. Subsequently, the blocking solution was removed, and the sections were incubated with the primary antibody (Phf11: pa5-76271, Invitrogen, USA, 1:1000) at 4 °C overnight. The sections were then washed three times with PBS and incubated with a secondary antibody (HRP-labeled goat anti-rabbit IgG, GB23303, Servicebio, China, 1:500). The sections were incubated for 50 min at room temperature, after which they were washed and incubated with TSA. Following this, the second primary and secondary antibodies were introduced separately for incubation (NF- κ Bp65: GB13142-1, Servicebio, 1:50; Alexa Fluor 488 labeled goat anti-rabbit IgG, GB25303, Servicebio, 1:400). All the sections were subsequently stained with DAPI for nuclear visualization. Images were captured using a fluorescence microscope (BX43F; U-HGLGPS; OLYMPUS, Japan).

2.11. *Cell culture and transfection*

Rat enteric glial cells (HZ-CRL-2690, ATCC, USA) were cultured in Dulbecco's modified Eagle's medium (DMEM; 11965092, Gibco, USA) containing 10% fetal bovine serum (FBS; F8318, Sigma-Aldrich, USA) and 1% penicillin and streptomycin (15140-122, Gibco, USA). The cells were maintained at 37 °C with 5% CO₂ under saturated humidity. Rat H9c2 cells were used as a positive reference to detect the basal expression of LOC108352929 and Phf11. Smart silencer technology was employed to knock down the expression of lncRNA LOC108352929 to observe its effect on the expression of Phf11, TNF- α , and IL-1 β in EGCs. EGCs were categorized into four groups: Smart Silencer-LOC108352929 group (SS), Smart Silencer-NC group (NC), transfected reagent control group (mock), and unprocessed cell control group (blank). Two replicate wells were used for each group. Smart silencer-LOC108352929 and Smart

silencer-NC were custom-synthesized by RIBOBIO (China). After 48 h of culture, cells were collected for RNA extraction.

2.12. Statistical analysis

Data analysis was conducted using SPSS 21.0 software. Intergroup comparisons of normally distributed data were performed using one-way ANOVA, with the choice between the least significant difference (LSD) method or Dunnett’s T3 method depending on the variance. Non-normally distributed data were compared between groups using non-parametric tests. $P < 0.05$ was considered as statistically significant.

3. Results

3.1. Moxibustion alleviates DSS-induced ulcerative colitis

The UC rat model was established by administering 4% DSS in drinking water, and the therapeutic effects of moxibustion were observed. The results demonstrated that rats in the NC group displayed normal activity and passed stools of moderate hardness and consistency. In contrast, rats in the UC group had loose and soft stools accompanied by mucus and blood. Compared with the UC group, rats in the MOX and SASP groups exhibited improved mobility, formed stools, and an absence of blood in their stool. Compared with the NC group, the DAI score was significantly increased in the UC group ($P < 0.05$). While, compared with the UC group [2.00 (1.00,

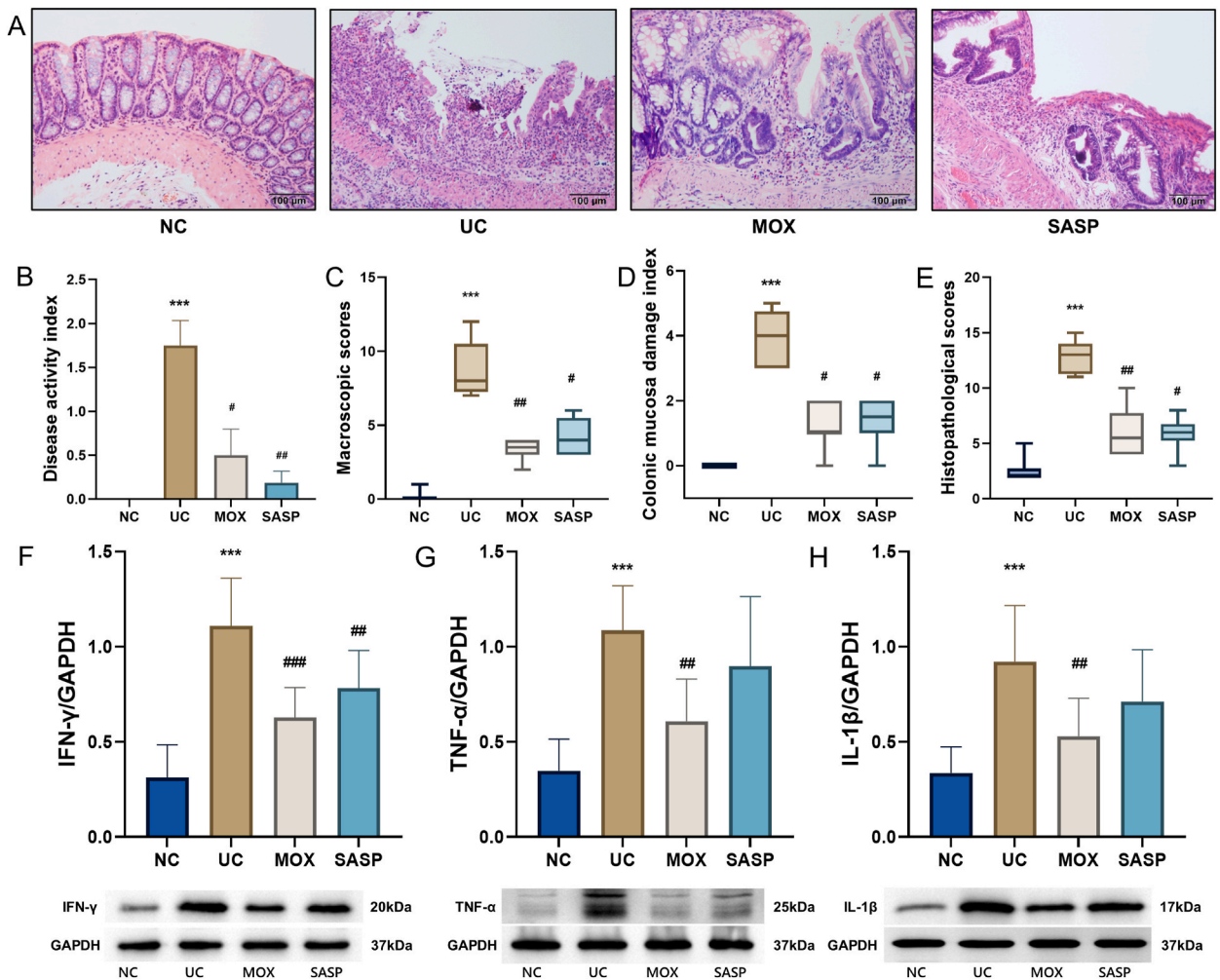


Fig. 2. Moxibustion alleviates DSS-induced colonic inflammation in UC rats. (A) H&E staining of the colon (magnification, $\times 200$); (B) Disease activity index; (C) Macroscopic score of rat colon tissue; (D) Colonic mucosa damage index; (E) Histopathological scores of the colon. Effects of moxibustion on the expression level of IFN- γ (F), TNF- α (G), and IL-1 β (H). Representative Western blot uncropped original scale images of Fig2 (F/G/H) were presented in Supplementary Fig. S1. Compared with the NC group, *** $P < 0.001$, compared with UC group, # $P < 0.05$, ## $P < 0.01$, ### $P < 0.001$, $n = 8$. NC: the normal control group; UC: the ulcerative colitis model group; MOX: the moxibustion group; SASP: the sulfasalazine group.

2.50)], DAI scores were significantly lower in MOX [0.25 (0.00, 0.50)] and SASP [0.00(0.00,0.38)] groups ($P < 0.05$) (Fig. 2B). Furthermore, the CMDI and macroscopic damage score of the rat colon were significantly reduced ($P < 0.05$) following MOX and SASP treatment (Fig. 2C and D).

HE staining revealed that the colonic mucosa in the UC group exhibited significant colonic epithelial damage, with extensive ulcers visible on the mucosa, notable changes in crypt architecture, a significant reduction in the number of crypts, a marked decrease in goblet cells, obvious bleeding, and extensive infiltration by inflammatory cells. The MOX group displayed repaired colonic epithelium, healing ulcers, changes in crypt architecture, decreasing crypt numbers and goblet cells, absent significant bleeding, and minimal inflammatory cell infiltration. In the SASP group, the colonic epithelium showed partial recovery, characterized by small mucosal ulcers, altered crypt structures, reduced goblet cells, and inflammatory cell infiltration (Fig. 2A). Compared with the NC group, the colon histopathology score was significantly increased in the UC group ($P < 0.05$); conversely, compared with the UC group [13.00 (11.25, 14.00)], histopathological scores were significantly lower in MOX [5.50 (4.00, 7.75)] and SASP [6.00(5.25,6.75)] groups ($P < 0.05$) (Fig. 2E). The scoring results are presented in Supplementary Table S4. These results suggested that MOX ameliorated colonic injury in DSS-induced UC rats.

To investigate the anti-inflammatory effects of moxibustion in UC rats, we further evaluated the expression levels of pro-inflammatory cytokines TNF- α , IFN- γ , and IL-1 β in the colonic tissues of rats in each group (Fig. 2F–H, Supplementary Fig. S1). The protein expression levels of TNF- α , IFN- γ , and IL-1 β were significantly higher in the UC group compared with the NC group ($P < 0.05$). Compared with the UC group, the levels of TNF- α , IFN- γ , and IL-1 β proteins were significantly reduced in the MOX group ($P < 0.05$), and the IFN- γ expression level was significantly decreased in the SASP group ($P < 0.05$). These results suggest that moxibustion can mitigate the overexpression of pro-inflammatory cytokines in the colon and ameliorate intestinal inflammation in UC rats.

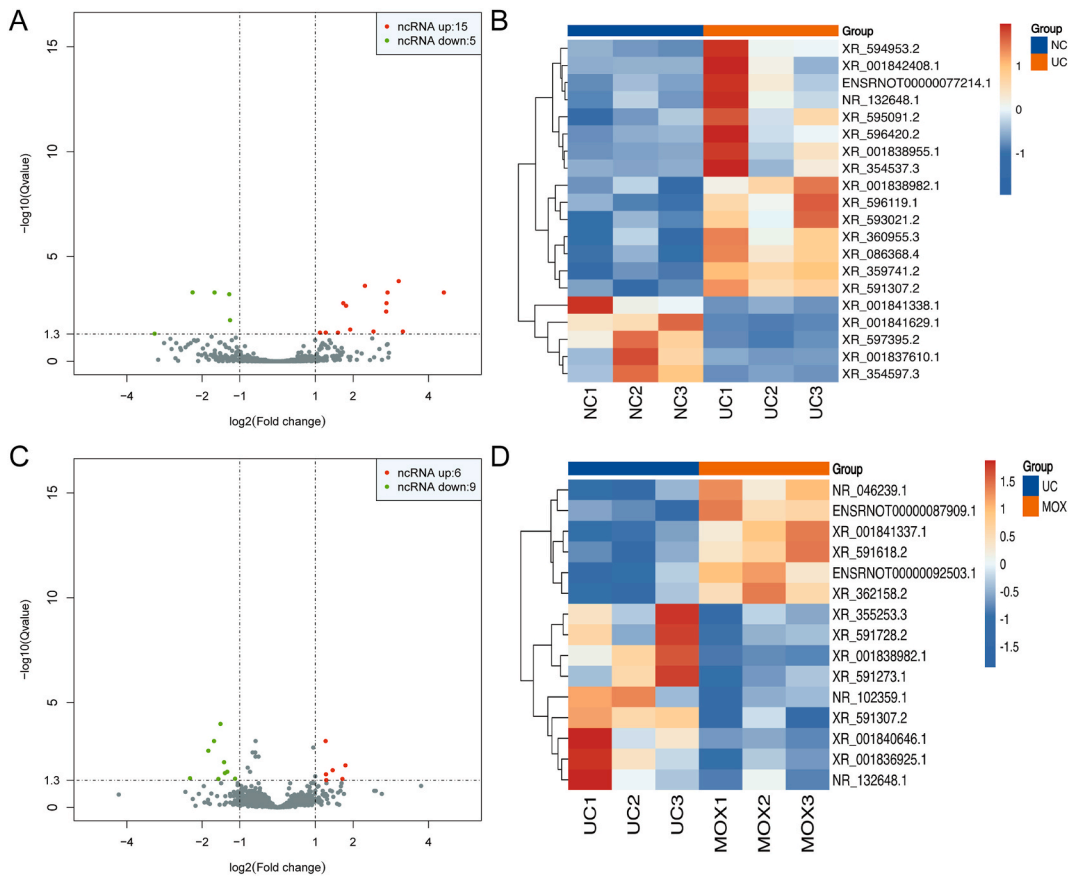


Fig. 3. RNA-seq identifies expression changes of lncRNAs in colon tissues. Volcano plots (A) and heat map (B) of differentially expressed lncRNAs between NC and UC group, Volcano plots(C) and heat map (D) of differentially expressed lncRNAs between UC and MOX group. Different expression lncRNA were identified with $|\log_2(\text{Fold Change})| > 1$ and P value < 0.05 ($n = 3$). Red dots in the volcano plot indicate upregulated ncRNAs and green dots indicate downregulated ncRNAs. Heatmap horizontal coordinates indicate samples, vertical coordinates indicate differential lncRNAs and the color from blue to red indicates that the expression level of lncRNAs ranges from low to high. NC: the normal control group; UC: the ulcerative colitis model group; MOX: the moxibustion group.

3.2. Moxibustion regulates lncRNA and mRNA expression profiles in colon tissues of UC rats

To further understand the mechanism by which moxibustion improves colonic inflammation in rats with UC, we used RNA-seq to analyze the expression profiles of colonic lncRNAs and mRNAs in NC, UC, and MOX groups. Data quality control (QC) revealed no significant fluctuations in base composition across the samples, and the QC results were satisfactory (Supplementary Fig. S2). Compared with the NC group, we observed 15 upregulated and 5 downregulated lncRNAs in the UC group (Fig. 3A and B, Table 1). When comparing the UC and MOX groups, we observed 6 upregulated and 9 downregulated lncRNAs in the MOX group (Fig. 3C and D, Table 2). Concerning mRNA expression profiles, 64 upregulated and 38 downregulated mRNAs were in the UC group compared to those in the NC group (Fig. 4A and B, Supplementary Table S5). However, following MOX intervention, we identified 117 upregulated and 40 downregulated mRNAs (Fig. 4C and D, Supplementary Table S6).

3.3. KEGG pathway analysis of differentially expressed mRNAs and differentially expressed lncRNA-targeted mRNAs

KEGG pathway analysis of differentially expressed mRNAs and differentially expressed lncRNA targeting mRNAs revealed the involvement of multiple KEGG pathways. Therefore, we only displayed the top 30 pathways with the most significant enrichment. Among these pathways, KEGG pathways associated with differentially expressed mRNAs between the NC and UC groups encompassed the AMPK signaling pathway, glycosaminoglycan biosynthesis (chondroitin sulfate/dermatan sulfate), glycosaminoglycan biosynthesis (keratan sulfate), glycosphingolipid biosynthesis (globo series), glycosphingolipid biosynthesis (ganglio series), fatty acid biosynthesis, adipocytokine signaling pathway, fatty acid degradation, glycerolipid metabolism, ABC transporters, and more (Fig. 5A). Furthermore, KEGG pathways linked to differentially expressed mRNAs between the UC and MOX groups included ubiquitin-mediated proteolysis, endocytosis, antigen processing and presentation, and cell adhesion molecules (Fig. 5B).

We analyzed KEGG signaling pathways associated with target mRNAs that were influenced by differentially expressed lncRNAs. The target mRNAs of the differentially expressed lncRNAs in the NC and UC groups were found to be predominantly enriched in pathways such as valine, leucine, and isoleucine degradation; intestinal immune network for IgA production; cysteine and methionine metabolism; tryptophan metabolism; tyrosine metabolism; pyruvate metabolism; ether lipid metabolism; chemokine signaling pathway; ribosome; nicotinate and nicotinamide metabolism; Jak-STAT signaling pathway; and Wnt signaling pathway (Fig. 6A). The target mRNAs of differentially expressed lncRNAs in the UC and MOX groups displayed significant enrichment in pathways including cell cycle, glycolysis/gluconeogenesis, glutathione metabolism, lysine degradation, fatty acid degradation, cysteine and methionine metabolism, ether lipid metabolism, tyrosine metabolism, endocytosis, cell adhesion molecules, and herpes simplex infection (Fig. 6B).

3.4. Screening and validation of differential lncRNA-mRNA interactions

lncRNAs primarily function by regulating the expression of target mRNAs. Predicting target mRNAs through the putative mechanisms of lncRNAs and establishing the relationship between differentially expressed lncRNAs and mRNAs are crucial for advancing our understanding of lncRNA functions. In this study, we investigated the biological functions of differentially expressed lncRNAs. To do so, we predicted both *cis*-regulated (in *cis*) and *trans*-regulated (in *trans*) target mRNAs for each differentially expressed lncRNA between the groups. The detailed results are presented in Supplementary Tables S7–S10.

We identified four pairs of key lncRNA-mRNAs under the condition that both the lncRNAs and their target mRNAs exhibited significant differences [$\log_2(\text{Fold Change}) > 1$ combined with $P < 0.05$]. These interactions include LOC103693584-Stxbp5l,

Table 1
Differentially expressed lncRNAs between the NC and UC groups.

lncRNA	Gene	Log ₂ FC	Regulation (UC/NC)
XR_359741.2	LOC102547136	3.209	up
XR_594953.2	LOC103693490	2.314	up
ENSRNOT00000077214.1	ENSRNOG00000058516.1	2.913	up
XR_001838955.1	LOC108351506	4.406	up
NR_132648.1	Hoxaas3	1.740	up
XR_596119.1	LOC102556949	2.886	up
XR_360955.3	LOC100910628	1.814	up
XR_354537.3	LOC102551142	2.877	up
XR_595091.2	LOC103693584	1.924	up
XR_001842408.1	LOC108348975	5.962	up
XR_593021.2	LOC103692634	2.541	up
XR_596420.2	LOC102557578	3.319	up
XR_001838982.1	LOC108351518	1.600	up
XR_086368.4	LOC688932	1.275	up
XR_591307.2	LOC102555028	1.122	up
XR_001841629.1	LOC108348398	-2.253	down
XR_001837610.1	LOC108350715	-1.671	down
XR_597395.2	LOC102550965	-1.281	down
XR_354597.3	Capn13	-1.260	down
XR_001841338.1	LOC102551046	-3.263	down

Table 2
Differentially expressed lncRNAs between the UC and MOX groups.

lncRNA	Gene	Log ₂ FC	Regulation (MOX/UC)
NR_046239.1	Rn45s	1.272	up
XR_001841337.1	LOC108352929	1.798	up
ENSRNOT00000087909.1	ENSRNOG00000058784.1	1.459	up
ENSRNOT00000092503.1	ENSRNOG0000000478.6	1.281	up
XR_591618.2	LOC102555456	1.717	up
XR_362158.2	LOC102554005	1.289	up
XR_591307.2	LOC102555028	-1.514	down
XR_001840646.1	LOC102551138	-1.685	down
XR_001836925.1	LOC102556058	-1.835	down
XR_001838982.1	LOC108351518	-1.418	down
NR_132648.1	Hoxaas3	-1.333	down
XR_355253.3	LOC102552770	-1.395	down
XR_591728.2	LOC103691914	-2.320	down
XR_591273.1	Prdx11l	-1.126	down
NR_102359.1	LOC100910802	-1.569	down

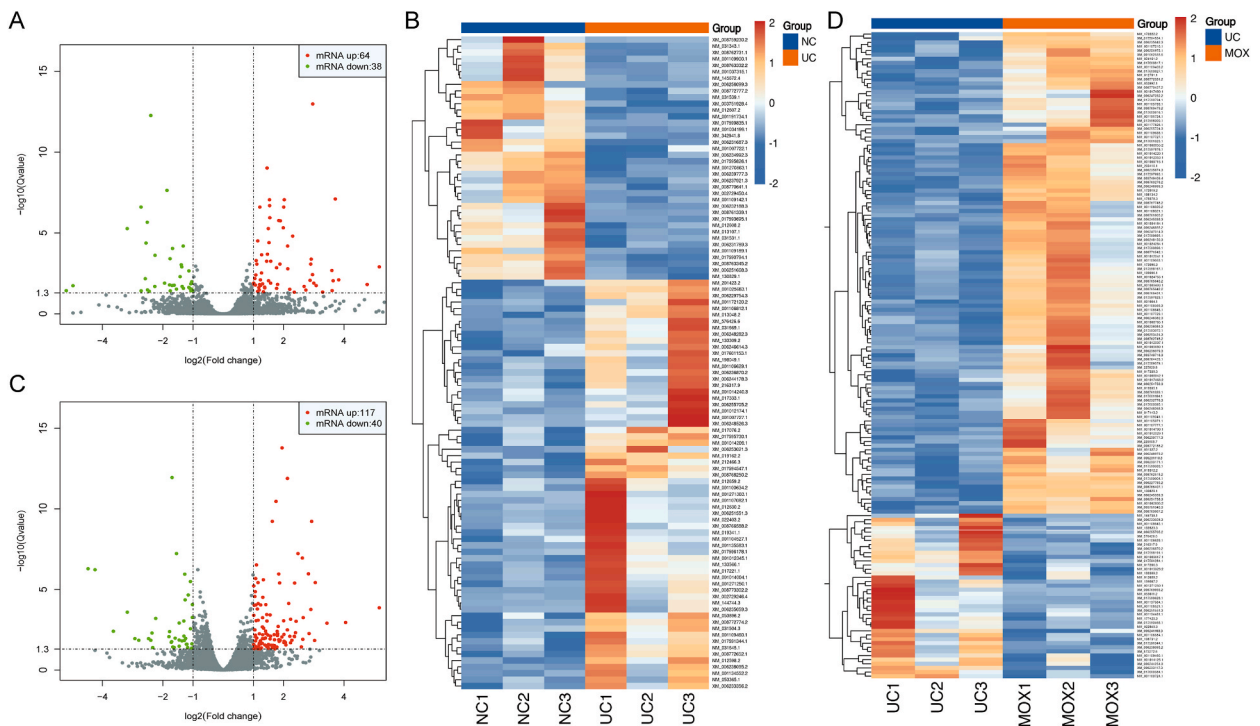


Fig. 4. RNA-seq identifies expression changes of mRNAs in colon tissues. Volcano plots (A) and heat map (B) of differentially expressed mRNAs between NC and UC group, Volcano plots (C) and heat map (D) of differentially expressed mRNAs between UC and MOX group. Different expression mRNA were identified with $|\log_2(\text{Fold Change})| > 1$ and P value < 0.05 ($n = 3$). Red dots in the volcano plot indicate upregulated ncRNAs and green dots indicate downregulated ncRNAs. Heatmap horizontal coordinates indicate samples, vertical coordinates indicate differential mRNAs and the color from blue to red indicates that the expression level of mRNAs ranges from low to high. NC: the normal control group; UC: the ulcerative colitis group; MOX: the moxibustion group.

LOC102547136-LOC102549235, LOC108352929-Phf11, and ENSRNOG00000058784.1-RT1-N3. To validate the lncRNA-mRNA expression within these four pairs, we performed RT-qPCR. The results indicated that LOC108352929-Phf11 displayed significant differences among the three groups, as illustrated in Fig. 7A and B. Specifically, when compared with the NC group, the expression of LOC108352929 was significantly lower in rats from the UC group ($P < 0.05$), whereas the mRNA expression of Phf11 was significantly higher ($P < 0.05$). However, compared with the UC group, the expression of LOC108352929 was significantly higher ($P < 0.05$) and the mRNA expression of Phf11 was significantly lower ($P < 0.05$) in rats from the MOX group.

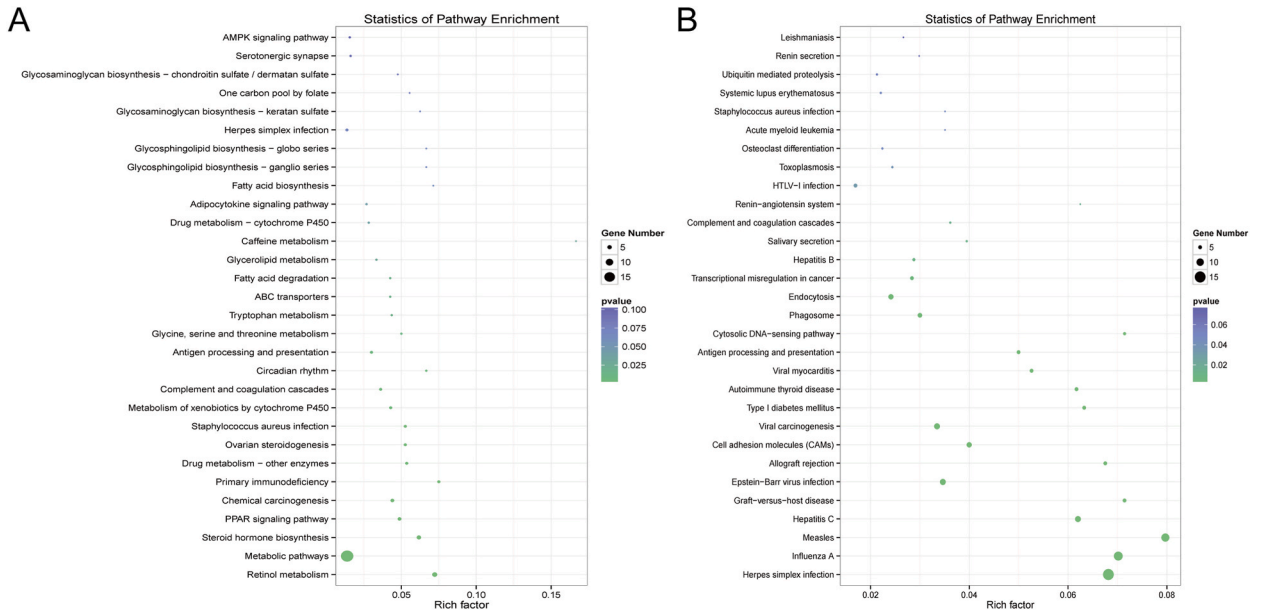


Fig. 5. KEGG pathway of different expressed mRNAs. (A) KEGG pathway of different expressed mRNAs between NC and UC group, (B) KEGG pathway of different expressed mRNAs between UC and MOX group. The horizontal coordinate indicates the proportion of target genes enriched to the pathway, and the vertical coordinate represents the pathway name. The size of the dots in the graph indicates the number of target genes enriched to the pathway, and the color indicates the P value.

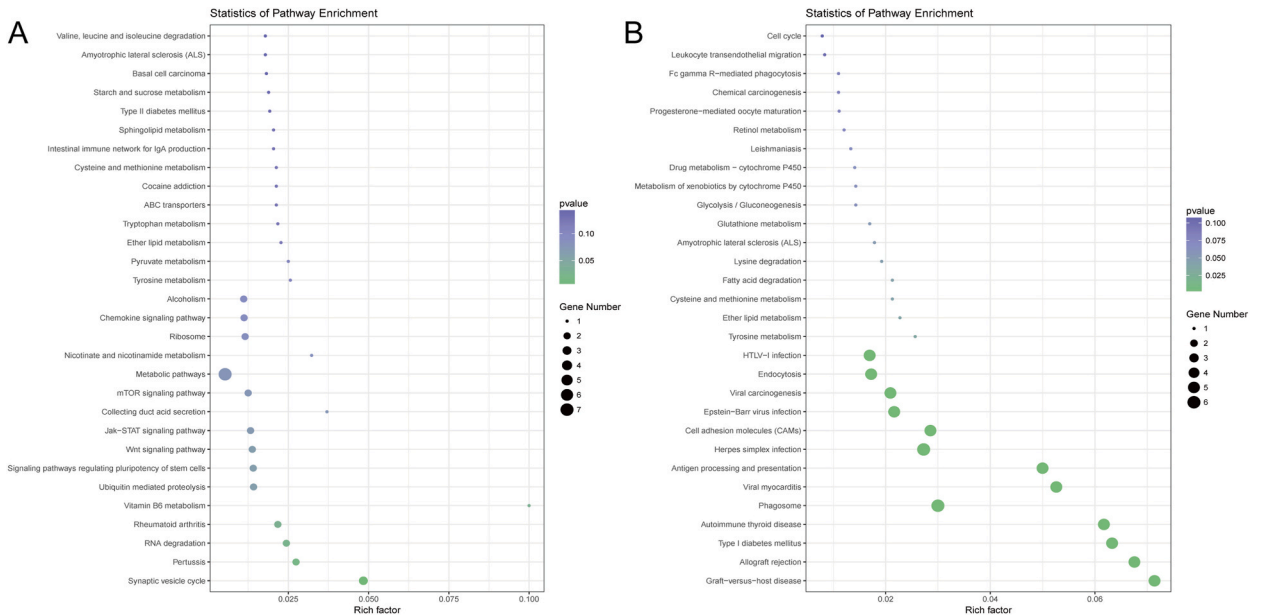


Fig. 6. KEGG pathway of different expressed lncRNA-targeted mRNAs. (A) KEGG pathway of different expressed lncRNA-targeted mRNAs between NC and UC group, (B) KEGG pathway of different expressed lncRNA-targeted mRNAs between UC and MOX group. The horizontal coordinate indicates the proportion of target genes enriched to the pathway, and the vertical coordinate represents the pathway name. The size of the dots in the graph indicates the number of target genes enriched to the pathway, and the color indicates the P value.

3.5. Effect of moxibustion on colonic Phf11-NF-κB expression in UC rats

Phf11 can interact with NF-κB, subsequently promoting IFN-γ expression and playing a pivotal role in regulating T cell activation [18]. Therefore, we employed immunofluorescence to scrutinize the co-localized expression of Phf11 and NF-κB in the colonic tissues of three rat groups, aiming to ascertain whether the therapeutic effect of moxibustion on UC was correlated with intestinal Phf11

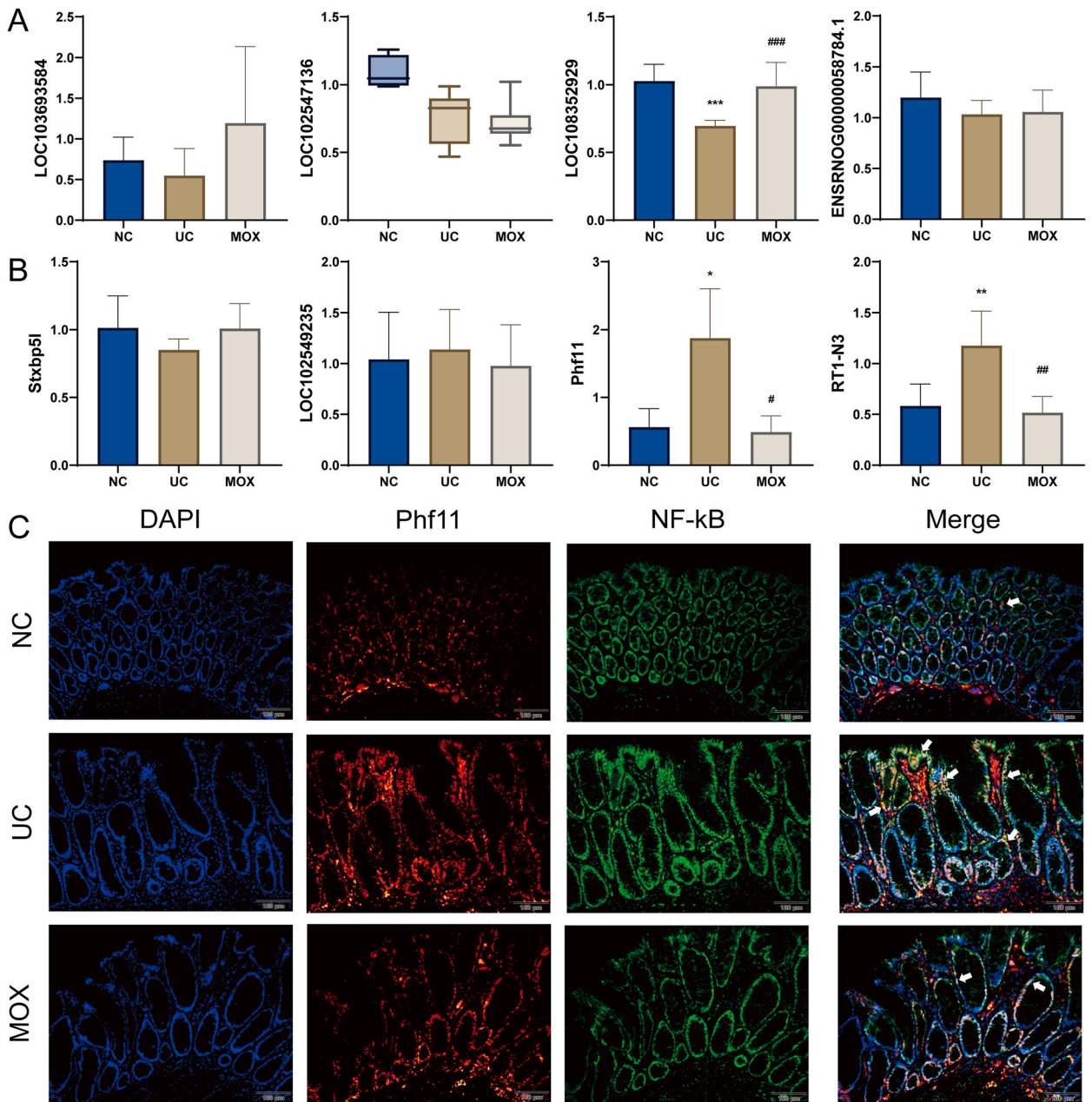


Fig. 7. Validation of lncRNA-mRNA expression level by using RT-qPCR. (A) Expression levels of lncRNA and (B) expression levels of mRNA in three groups. (C) Phf11 and NF-κB expression and co-localization in rat colon (magnification, $\times 200$). NC: the normal control group; UC: the ulcerative colitis model group; MOX: the moxibustion group. Compared with NC group, $**P < 0.01$, $***P < 0.001$; compared with UC group, $\#P < 0.05$, $\#\#P < 0.01$, $\#\#\#P < 0.001$, $n = 6$.

expression. Compared with the NC group, there was an increase in the positive expression and co-localization of Phf11 and NF-κB. However, moxibustion treatment led to a reduction in the expression and colocalization of Phf11 and NF-κB (Fig. 7C). These findings imply that the inhibition of Phf11 overexpression in the rat intestine may be one of the mechanisms by which moxibustion ameliorates intestinal inflammation in UC.

3.6. Effect of LOC108352929 knockdown on TNF- α expression in rat EGCs

To assess the basal expression of LOC108352929 and Phf11 in rat enteric glial cells (EGCs), we used rat H9c2 cells as a comparison. The expression of these transcripts met the conditions for conducting long non-coding RNA interference (lncRNA RNAi) experiments

Fig. 8. Effect of knockdown of LOC108352929 on TNF- α mRNA expression in rat EGCs. (A) LOC108352929 and Phf11 expression in EGC and H9c2 cells, (B) LOC108352929 and Phf11 mRNA expression in each group of cells after interfering with the expression of LOC108352929, (C) mRNA levels of TNF- α and IL-1 β in each group of cells after LOC108352929 interference. (D) Venn diagram displaying the miRNA prediction results for LOC108352929. (E) Construction of the network involving target genes and candidate miRNAs. (F) Formation of the LOC108352929-miRNA-Phf11 network. In the diagram, red circles represent lncRNAs, green circles represent mRNAs, and yellow diamonds represent common target miRNAs. NC: transfected Smart Silencer - NC group; SS: transfected Smart Silencer - LOC108352929 group; mock: transfected reagent control group; blank: unprocessed cell control group. Compared with the NC group, * $P < 0.05$.

(Fig. 8A). Subsequently, we employed RNAi technology (Smart Silencer) to transfect rat EGCs, which resulted in a significant reduction in the transcript levels of lncRNA LOC108352929 ($P < 0.05$) with a silencing efficiency of approximately 30%. However, no significant intergroup differences were noted in the mRNA expression level of Phf11 (Fig. 8B). We also examined the expression levels of TNF- α and IL-1 β . The results indicated a significant increase in TNF- α mRNA expression following the knockdown of lncRNA LOC108352929 compared to the NC group ($P < 0.05$), while the expression level of IL-1 β mRNA remained unchanged (Fig. 8C). These results suggest that moxibustion improves the level of intestinal inflammation in rats with UC, which may be partially related to the promotion of LOC108352929 expression.

After the knockdown of LOC108352929 expression in cellular experiments, it resulted in a significant increase in TNF- α , while no notable effect on Phf11 mRNA expression was observed. This led us to speculate that miRNAs may play a role in the intricate interaction between lncRNAs and mRNAs. Consequently, we constructed a LOC108352929-miRNA-Phf11 interaction network (Fig. 8D–F). These results indicated that 30 miRNAs, including rno-miR-153-5p, rno-miR-877, and rno-miR-3557-3p, could potentially mediate the competitive inhibitory relationship between LOC108352929 and Phf11.

4. Discussion

Ulcerative colitis (UC) is a chronic, recurrent inflammatory bowel disease that primarily affects the mucosa and submucosa of the rectum and colon. Moxibustion, a traditional Chinese medicine therapy, has demonstrated clinical effectiveness in treating UC and improving psychological well-being, including anxiety and depression, as well as the overall quality of life of patients [19,20]. Our observations revealed that moxibustion not only enhanced colonic DAI, CMDI, macroscopic, and histopathological scores but also alleviated colonic injury in DSS-induced UC model rats, consistent with our previous research [8,14,21]. The HE results indicated that in the MOX group, despite a reduction in goblet cells and the presence of inflammatory cell infiltration, there was observed restoration in the colonic epithelium compared to the UC group. Although the pathogenesis of UC remains unclear, intestinal mucosal immune dysregulation is widely believed to play a pivotal role in its development [22]. Immune activation within the colonic mucosa leads to the production of numerous inflammatory cytokines, resulting in the heightened expression of pro-inflammatory factors, such as TNF- α , IFN- γ , IL-1 β , IL-6, and IL-13 in the colons of UC-afflicted rats [23,24]. In this study, we observed that moxibustion significantly reduced colonic protein expression levels of TNF- α , IFN- γ , and IL-1 β in UC rats, contributing to the amelioration of UC-associated colonic inflammation.

lncRNAs play crucial roles in various biological processes by regulating gene expression and serve as significant contributors to the pathogenesis and progression of numerous diseases [25–27]. Therefore, lncRNAs have potential utility as biomarkers or therapeutic targets for UC. In clinical samples obtained from patients with UC and healthy populations, 99 differentially expressed lncRNAs were identified, underscoring the substantial role of lncRNAs in UC pathogenesis and inflammatory response [28]. In this study, we conducted RNA-seq analysis on colon tissues from rats in the normal, model, and moxibustion groups to delineate alterations in lncRNA and mRNA expression within the colon tissues of these groups. We aimed to identify the potential lncRNA targets influenced by moxibustion treatment in UC. Within the NC and UC groups, we identified 20 differentially expressed (DE) lncRNAs (15 upregulated and 5 downregulated) and 102 DE mRNAs (64 upregulated and 38 downregulated). In UC and MOX tissues, we identified 15 DE lncRNAs (6 upregulated and 9 downregulated) and 157 DE mRNAs (117 upregulated and 40 downregulated).

We conducted KEGG analysis of DE mRNAs and lncRNA target mRNAs. The DE mRNAs and DE lncRNA target mRNAs in UC and NC rats were found to be significantly enriched in pathways related to amino acid metabolism, particularly tryptophan (TRP) metabolism. The progression of UC is intricately linked to disruptions in amino acid metabolism, and rebalancing these pathways can help suppress intestinal inflammation and enhance the function of the intestinal barrier in UC [29,30]. Tryptophan is one of the eight essential amino acids found in humans. The metabolism in the intestine involves interactions between intestinal epithelial cells and microorganisms [31]. Notably, patients with IBD exhibit significantly reduced serum TRP levels, which are negatively correlated with disease activity and CRP levels [32]. TRP can alleviate intestinal inflammation by restoring intestinal barrier integrity and modulating the intestinal microbiota [33,34]. In a previously published review, our team emphasized the crucial role of the TRP metabolic pathway in IBD-related depression [35]. Furthermore, the target mRNAs of the differentially expressed lncRNAs between the NC and UC groups and between the MOX and UC groups were significantly enriched in amino acid metabolism-related pathways, including cysteine and methionine metabolism, ether lipid metabolism, and tyrosine metabolism. Cysteine and methionine belong to a group of sulfur-containing amino acids that are notably susceptible to oxidation because of the electron-rich sulfur atoms in their side chains [36]. Methionine can also be converted into cysteine *via* the transsulfuration pathway [37]. An increase in the levels of these amino acids in the gastrointestinal tract leads to a dose-dependent escalation of colonic inflammation [38]. The findings of this study further suggest that the metabolism of cysteine and methionine may represent one of the key pathways through which moxibustion ameliorates inflammation in the intestinal tract of rats with UC.

Increasing evidence suggests that specific lncRNAs and their downstream signaling pathways play crucial roles in inflammation and

maintenance of the intestinal barrier in ulcerative colitis (UC). For instance, Zhu found that lncRNA MALAT1 was upregulated in the colonic tissues of UC patients, and promoted lipopolysaccharide (LPS)-induced inflammatory responses [39]. Tian discovered that lncRNA CDKN2B-AS1 could negatively regulate miR-16-5p and miR-195-5p levels and inhibit serum inflammatory cytokine TNF- α , IL-6, and sIL-2R levels in UC patients [40]. Furthermore, inhibition of lncRNA-NEAT1 affects glucose metabolism in intestinal epithelial cells by modulating its downstream target LDHA via miR-410-3p, resulting in intestinal epithelial cell dysfunction in ulcerative colitis [41]. In this study, we identified four pairs of differentially expressed lncRNA-mRNAs using screening conditions in which both lncRNAs and their target mRNAs exhibited significant differences between the groups. We assessed their expression levels using RT-qPCR, which revealed significant intergroup differences in LOC108352929 and Phf11. Although there is limited research on the function of LOC108352929, Phf11 is known to have a wide range of functions in promoting T-cell activation and viability. In Th1 cells, Phf11 interacts with NF- κ B to activate IL-2 and IFN- γ transcription [18]. In this study, we also observed increased expression of Phf11 and NF- κ B in the colonic tissues of UC rats, and moxibustion effectively suppressed their expression and co-localization.

To gain a deeper understanding of the function of LOC108352929, we used RNAi to interfere with its expression in rat enteric glial cells. Following the inhibition of LOC108352929, the expression of TNF- α mRNA significantly increased, while no significant difference was observed in Phf11 expression. This suggests that LOC108352929 may mitigate intestinal inflammation by suppressing TNF- α expression.

miRNAs are small non-coding RNAs that inhibit mRNA translation and promote mRNA degradation [42]. In contrast, lncRNAs modulate target mRNA expression by acting as sponges that adsorb miRNAs [43]. We considered whether the lack of significant change in Phf11 expression following LOC108352929 inhibition was related to miRNAs. Consequently, we constructed the LOC108352929-miRNA-Phf11 network and identified 30 miRNAs that may play central roles, including miR-378a-5p and miR-200b-3p. For instance, miR-378a-5p, a highly expressed miRNA in human umbilical cord mesenchymal stem cell (hucMSC)-derived exosomes, has been found to target NLRP3, inhibit NLRP3 inflammatory vesicles and prevent cellular pyroptosis, thereby facilitating the repair of DSS-induced colitis [44]. Similarly, miR-200b-3p regulates the composition of the microbiota and contributes to the maintenance of intestinal barrier integrity [45]. When miR-200b-3p levels were inhibited, the disease activity index in UC rats increased, whereas the upregulation of miR-200b-3p mitigated inflammation and apoptosis in colonic epithelial cells in UC rats [46]. These findings suggest that multiple UC-related miRNAs are involved in the interactions between LOC108352929 and Phf11.

In addition, this study had some limitations. In this study, we conclude that the interaction between LOC108352929 and Phf11 may play an important role in the improvement of UC by moxibustion. We used RNA-seq, bioinformatic analysis, RT-qPCR, immunofluorescence staining, and smart silencing technology to explore the relationship between LOC108352929 and Phf11. Although we observed moxibustion regulatory of LOC108352929-Phf11 and co-expression of Phf11 and NF- κ B in the colon of UC rats, only its regulatory effect on TNF- α was observed after knockdown of LOC108352929 expression in rat EGCs. Further silencing of LOC108352929 *in vivo* would provide more comprehensive evidence effectiveness of moxibustion in DSS-induced colitis.

5. Conclusions

In conclusion, moxibustion ameliorated intestinal mucosal injury and alleviated intestinal inflammation in UC rats. The mechanism may be related to the regulation of lncRNA expression profiles, modulation of LOC108352929-Phf11 expression, and the reduction of TNF- α and other pro-inflammatory factors' expression.

Ethics statement

This study was reviewed and approved by Animal Ethics Committee of the Shanghai University of Traditional Chinese Medicine, with the approval number: [PZSHUTCM200209001].

Funding statement

This research was funded by the National Natural Science Foundation of China (81973953, 82274641) and Natural Science Foundation of Shanghai Municipality, China (21ZR1460200 and 22ZR1458400).

Data availability statement

Data included in article/supp. material/referenced in article.

CRediT authorship contribution statement

Guona Li: Writing – original draft, Methodology, Data curation. **Chen Zhao:** Conceptualization. **Jing Xu:** Writing – review & editing, Methodology. **Yan Huang:** Writing – review & editing. **Yu Qiao:** Methodology. **Feng Li:** Methodology. **Guangbin Peng:** Methodology. **Shiyu Zheng:** Writing – review & editing. **Lu Zhu:** Data curation. **Ling Yang:** Writing – review & editing. **Zhaoqin Wang:** Methodology, Data curation. **Huangan Wu:** Conceptualization.

Declaration of competing interest

The authors declare that they have no known competing financial interests or personal relationships that could have appeared to influence the work reported in this paper.

Acknowledgments

The authors thank RIBOBIO (China) for the help with custom synthesized Smart silencer-LOC108352929 and Smart silencer-NC. We also thank Elsevier for providing language editing services for this article. The image material of the rat in Fig. 1 was obtained from *biorender.com*. (Agreement number: FX261ZSG5E).

Appendix A. Supplementary data

Supplementary data to this article can be found online at <https://doi.org/10.1016/j.heliyon.2024.e26898>.

References

- [1] T. Kobayashi, B. Siegmund, C. Le-Berre, S.C. Wei, M. Ferrante, B. Shen, C.N. Bernstein, S. Danese, L. Peyrin-Biroulet, T. Hibi, Ulcerative colitis, *Nat. Rev. Dis. Prim.* 6 (2020) 74.
- [2] L. Du, C. Ha, Epidemiology and pathogenesis of ulcerative colitis, *Gastroenterol. Clin. N. Am.* 49 (2020) 643–654.
- [3] S.-C. Wei, J. Sollano, Y.T. Hui, W. Yu, P.V. Santos Estrella, L.J.Q. Llamado, N. Koram, Epidemiology, burden of disease, and unmet needs in the treatment of ulcerative colitis in Asia, *Exp. Rev. Gastroenterol. Hepatol.* 15 (2021) 275–289.
- [4] H. Geng, X.-D. Tan, Functional diversity of long non-coding RNAs in immune regulation, *Genes Dis* 3 (2016) 72–81.
- [5] Y.-X. Wang, C. Lin, L.-J. Cui, T.-Z. Deng, Q.-M. Li, F.-Y. Chen, X.-P. Miao, Mechanism of M2 macrophage-derived extracellular vesicles carrying lncRNA MEG3 in inflammatory responses in ulcerative colitis, *Bioengineered.* 12 (n.d.) 12722–12739.
- [6] A.H. Mirza, C.H. Berthelsen, S.E. Seemann, X. Pan, K.S. Frederiksen, M. Vilien, J. Gorodkin, F. Pociot, Transcriptomic landscape of lncRNAs in inflammatory bowel disease, *Genome Med.* 7 (2015) 39.
- [7] Y. Wang, N. Wang, L. Cui, Y. Li, Z. Cao, X. Wu, Q. Wang, B. Zhang, C. Ma, Y. Cheng, Long non-coding RNA MEG3 alleviated ulcerative colitis through upregulating miR-98-5p-Sponged IL-10, *Inflammation* 44 (2021) 1049–1059.
- [8] D. Zhang, Y.-B. Ren, K. Wei, J. Hong, Y.-T. Yang, L.-J. Wu, J. Zhang, Z. Shi, H.-G. Wu, X.-P. Ma, Herb-partitioned moxibustion alleviates colon injuries in ulcerative colitis rats, *World J. Gastroenterol.* 24 (2018) 3384–3397.
- [9] H.-G. Wu, L.-B. Zhou, D.-R. Shi, S.-M. Liu, H.-R. Liu, B.-M. Zhang, H.-P. Chen, L.-S. Zhang, Morphological study on colonic pathology in ulcerative colitis treated by moxibustion, *World J. Gastroenterol.* 6 (2000) 861–865.
- [10] X.-J. Wang, X.-Y. Li, X.-C. Guo, L. Liu, Y.-Y. Jin, Y.-Q. Lu, Y.-J.-N. Cao, J.-Y. Long, H.-G. Wu, D. Zhang, G. Yang, J. Hong, Y.-T. Yang, X.-P. Ma, lncRNA-miRNA-mRNA network analysis Reveals the potential biomarkers in Crohn's disease rats treated with herb-partitioned moxibustion, *J. Inflamm. Res.* 15 (2022) 1699–1716.
- [11] Y. Li, P. Yang, F. Chen, J. Tang, Z. He, Z. Yang, L. Weng, J. Guo, L. Zeng, H. Yin, Ccr12-centred immune-related lncRNA-mRNA co-expression network revealed the local skin immune activation mechanism of moxibustion on adjuvant arthritis mice, *Life Sci.* 329 (2023) 121910.
- [12] Y. Huang, Z. Ma, Y.-H. Cui, H.-S. Dong, J.-M. Zhao, C.-Z. Dou, H.-R. Liu, J. Li, H.-G. Wu, Effects of herb-partitioned moxibustion on the miRNA expression profiles in colon from rats with DSS-induced ulcerative colitis, *Evid Based Complement Alternat Med* 2017 (2017) 1767301.
- [13] S.-Y. Xu, R.-L. Bian, X. Chen, *Methodology of Pharmacological Experiments*, third ed., People's Medical Publishing House, Beijing, 2002, p. 203.
- [14] Q. Qi, Y.-N. Liu, S.-Y. Lv, H.-G. Wu, L.-S. Zhang, Z. Cao, H.-R. Liu, X.-M. Wang, L.-Y. Wu, Gut microbiome alterations in colitis rats after moxibustion at bilateral Tianshu acupoints, *BMC Gastroenterol.* 22 (2022) 62.
- [15] J.-W. Mao, X.-M. He, H.-Y. Tang, Y.-D. Wang, Protective role of metalloproteinase inhibitor (AE-941) on ulcerative colitis in rats, *World J. Gastroenterol.* 18 (2012) 7063–7069.
- [16] J.Y. Yao, Y. Lu, M. Zhi, C.J. Li, P.J. Hu, X. Gao, Inhibition of the interleukin-23/interleukin-17 pathway by anti-interleukin-23p19 monoclonal antibody attenuates 2,4,6-trinitrobenzene sulfonic acid-induced Crohn's disease in rats, *Mol. Med. Rep.* 10 (2014) 2105–2110.
- [17] J. Fichna, M. Dickey, K. Lewellyn, A. Janecka, J.K. Zjawiony, W.K. MacNaughton, M.A. Storr, Salvinorin A has anti-inflammatory and antinociceptive effects in experimental models of colitis in mice mediated by KOR and CB1 receptors, *Inflamm. Bowel Dis.* 18 (2012) 1137–1145.
- [18] N. Rahman, G. Stewart, G. Jones, A role for the atopy-associated gene PHLF11 in T-cell activation and viability, *Immunol. Cell Biol.* 88 (2010) 817–824.
- [19] Q. Qi, H. Im, K.-S. Li, M. Gu, H.-G. Wu, L. Yang, Y. Huang, J.-M. Zhao, Y.-H. Cui, H.-R. Liu, L.-Y. Wu, Influence of herb-partitioned moxibustion at Qihai (CV6) and bilateral Tianshu (ST25) and Shangjuxu (ST37) acupoints on toll-like receptors 4 signaling pathways in patients with ulcerative colitis, *J. Tradit. Chin. Med.* 41 (2021) 479–485.
- [20] Y.-Y. Lin, J.-M. Zhao, Y.-J. Ji, Z. Ma, H.-D. Zheng, Y. Huang, Y.-H. Cui, Y. Lu, H.-G. Wu, Typical ulcerative colitis treated by herbs-partitioned moxibustion: a case report, *World J Clin Cases* 8 (2020) 1515–1524.
- [21] Q. Qi, R. Zhong, Y.-N. Liu, C. Zhao, Y. Huang, Y. Lu, Z. Ma, H.-D. Zheng, L.-Y. Wu, Mechanism of electroacupuncture and herb-partitioned moxibustion on ulcerative colitis animal model: a study based on proteomics, *WJG* 28 (2022) 3644–3665.
- [22] V. Mitsialis, S. Wall, P. Liu, J. Ordovas-Montanes, T. Parmet, M. Vukovic, D. Spencer, M. Field, C. McCourt, J. Toothaker, A. Bousvaros, A.K. Shalek, L. Kean, B. Horwitz, J. Goldsmith, G. Tseng, S.B. Snapper, L. Konnikova, Single-cell Analyses of colon and blood reveal Distinct immune cell Signatures of ulcerative colitis and Crohn's disease, *Gastroenterology* 159 (2020) 591–608.e10.
- [23] X. Li, X. Wu, Q. Wang, W. Xu, Q. Zhao, N. Xu, X. Hu, Z. Ye, S. Yu, J. Liu, X. He, F. Shi, Q. Zhang, W. Li, Sanguinarine ameliorates DSS induced ulcerative colitis by inhibiting NLRP3 inflammasome activation and modulating intestinal microbiota in C57BL/6 mice, *Phytomedicine* 104 (2022) 154321.
- [24] F. Zhu, J. Zheng, F. Xu, Y. Xi, J. Chen, X. Xu, Resveratrol alleviates dextran sulfate sodium-induced acute ulcerative colitis in mice by mediating PI3K/Akt/VEGFA pathway, *Front. Pharmacol.* 12 (2021) 693982.
- [25] Y.-T. Tan, J.-F. Lin, T. Li, J.-J. Li, R.-H. Xu, H.-Q. Ju, lncRNA-mediated posttranslational modifications and reprogramming of energy metabolism in cancer, *Cancer Commun.* 41 (2021) 109–120.
- [26] J.M. Engreitz, J.E. Haines, E.M. Perez, G. Munson, J. Chen, M. Kane, P.E. McDonel, M. Guttman, E.S. Lander, Local regulation of gene expression by lncRNA promoters, transcription and splicing, *Nature* 539 (2016) 452–455.
- [27] A.B. Herman, D. Tsitsipatis, M. Gorospe, Integrated lncRNA function upon Genomic and Epigenomic regulation, *Mol Cell* 82 (2022) 2252–2266.
- [28] M.K. Ray, C.G. Fenton, R.H. Paulsen, Novel long non-coding RNAs of relevance for ulcerative colitis pathogenesis, *Noncoding RNA Res* 7 (2022) 40–47.

- [29] M. Liu, Y. Wang, H. Xiang, M. Guo, S. Li, M. Liu, J. Yao, The tryptophan metabolite Indole-3-Carboxaldehyde alleviates mice with DSS-induced ulcerative colitis by Balancing amino acid metabolism, inhibiting intestinal inflammation, and improving intestinal barrier function, *Molecules* 28 (2023) 3704.
- [30] C. Liu, C. Sun, Y. Cheng, β -Glucan alleviates mice with ulcerative colitis through interactions between gut microbes and amino acids metabolism, *J. Sci. Food Agric.* 103 (2023) 4006–4016.
- [31] A. Agus, J. Planchais, H. Sokol, Gut Microbiota Regulation of Tryptophan Metabolism in Health and Disease, *Cell Host Microbe* 23 (2018) 716–724.
- [32] S. Nikolaus, B. Schulte, N. Al-Massad, F. Thieme, D.M. Schulte, J. Bethge, A. Rehman, F. Tran, K. Aden, R. Häsler, N. Moll, G. Schütze, M.J. Schwarz, G. H. Waetzig, P. Rosenstiel, M. Krawczak, S. Szymczak, S. Schreiber, Increased tryptophan metabolism is associated with activity of inflammatory bowel diseases, *Gastroenterology* 153 (2017) 1504–1516.e2.
- [33] S.A. Scott, J. Fu, P.V. Chang, Microbial tryptophan metabolites regulate gut barrier function via the aryl hydrocarbon receptor, *Proc. Natl. Acad. Sci. U. S. A.* 117 (2020) 19376–19387.
- [34] X.-J. Zhang, Z.-W. Yuan, C. Qu, X.-T. Yu, T. Huang, P.V. Chen, Z.-R. Su, Y.-X. Dou, J.-Z. Wu, H.-F. Zeng, Y. Xie, J.-N. Chen, Palmatine ameliorated murine colitis by suppressing tryptophan metabolism and regulating gut microbiota, *Pharmacol. Res.* 137 (2018) 34–46.
- [35] L.-M. Chen, C.-H. Bao, Y. Wu, S.-H. Liang, D. Wang, L.-Y. Wu, Y. Huang, H.-R. Liu, H.-G. Wu, Tryptophan-kynurenine metabolism: a link between the gut and brain for depression in inflammatory bowel disease, *J. Neuroinflammation* 18 (2021) 135.
- [36] B. Ezraty, A. Gennaris, F. Barras, J.-F. Collet, Oxidative stress, protein damage and repair in bacteria, *Nat. Rev. Microbiol.* 15 (2017) 385–396.
- [37] P.S. Upadhyayula, D.M. Higgins, A. Mela, M. Banu, A. Dovas, F. Zandkarimi, P. Patel, A. Mahajan, N. Humala, T.T.T. Nguyen, K.R. Chaudhary, L. Liao, M. Argenziano, T. Sudhakar, C.P. Sperring, B.L. Shapiro, E.R. Ahmed, C. Kinslow, L.F. Ye, M.D. Siegelin, S. Cheng, R. Soni, J.N. Bruce, B.R. Stockwell, P. Canoll, Dietary restriction of cysteine and methionine sensitizes gliomas to ferroptosis and induces alterations in energetic metabolism, *Nat. Commun.* 14 (2023) 1187.
- [38] J. Stavsky, R. Maitra, The Synergistic role of Diet and Exercise in the prevention, pathogenesis, and management of ulcerative colitis: an underlying metabolic mechanism, *Nutr. Metab. Insights* 12 (2019) 1178638819834526.
- [39] M. Zhu, J. Xie, LncRNA MALAT1 promotes ulcerative colitis by upregulating lncRNA ANRIL, *Dig. Dis. Sci.* 65 (2020) 3191–3196.
- [40] Y. Tian, L. Cui, C. Lin, Y. Wang, Z. Liu, X. Miao, LncRNA CDKN2B-AS1 relieved inflammation of ulcerative colitis via sponging miR-16 and miR-195, *Int. Immunopharm.* 88 (2020) 106970.
- [41] S. Ni, Y. Liu, J. Zhong, Y. Shen, Inhibition of LncRNA-NEAT1 alleviates intestinal epithelial cells (IECs) dysfunction in ulcerative colitis by maintaining the homeostasis of the glucose metabolism through the miR-410-3p-LDHA axis, *Bioengineered.* 13 (n.d.) 8961–8971.
- [42] M. Correia de Sousa, M. Gjorgjieva, D. Dolicka, C. Sobolewski, M. Foti, Deciphering miRNAs' action through miRNA editing, *Int. J. Mol. Sci.* 20 (2019) 6249.
- [43] I. Samoilă, S. Dinescu, M. Costache, Interplay between cellular and molecular mechanisms underlying inflammatory bowel diseases development-A focus on ulcerative colitis, *Cells* 9 (2020) 1647.
- [44] X. Cai, Z. Zhang, J. Yuan, D.K.W. Ocansey, Q. Tu, X. Zhang, H. Qian, W. Xu, W. Qiu, F. Mao, hucMSC-derived exosomes attenuate colitis by regulating macrophage pyroptosis via the miR-378a-5p/NLRP3 axis, *Stem Cell Res. Ther.* 12 (2021) 416.
- [45] Q. Shen, Z. Huang, L. Ma, J. Yao, T. Luo, Y. Zhao, Y. Xiao, Y. Jin, Extracellular vesicle miRNAs promote the intestinal microenvironment by interacting with microbes in colitis, *Gut Microb.* 14 (2022) 2128604.
- [46] C. Zheng, T. Lu, Z. Fan, miR-200b-3p alleviates TNF- α -induced apoptosis and inflammation of intestinal epithelial cells and ulcerative colitis progression in rats via negatively regulating KHDRBS1, *Cytotechnology* 73 (2021) 727–743.